High Performance Cobotics

Eric L. Faulring, J. Edward Colgate and Michael A. Peshkin, *Members, IEEE*

***Abstract*— Cobots are a class of robots that use continuously variable transmissions to develop high fidelity programmable constraint surfaces. Cobots consume very little electrical power even when providing high output forces, and their transmissions are highly efficient across a broad range of transmission ratios. Cobotic transmissions also have the ability to act either as a brake or to become entirely free. The design and performance of the Cobotic Hand Controller, a recently developed six-degree-of-freedom haptic display, is reviewed. This device illustrates the high dynamic range and low power consumption achievable by cobots. A thorough comparison of the power efficiency of a cobotic system versus a conventional electro-mechanical system is provided.**

I. Introduction

Three key requirements of robotic technologies used for prosthetics and rehabilitation are low weight, low power consumption and safety. We propose cobotic technology as a transmission architecture that can address all of these issues. Cobots are robots that utilize the nonholonomic constraints of steered wheels to relate the relative velocities of mechanism links. A cobotic transmission is a continuously variable transmission (CVT) between positive and negative ratios, and can relate two translational velocities, two rotational velocities, or a rotational velocity to a translational velocity [1]. We have recently introduced the Cobotic Hand Controller (Figure 1), a six-degree-of-freedom powered cobot, and described its capabilities as a haptic interface [2, 3]. Through the course of this paper, we demonstrate that the mechanical architecture and transmissions used in the Cobotic Hand Controller address all three of the above mentioned requirements of robotics for prosthetics and rehabilitation.

Cobotic technology provides a highly power and weight efficient transmission architecture that can have minimal dissipation and trivial dynamics. Gear trains, timing belt transmissions, hydraulic and pneumatic systems as well as cable systems all have dissipative losses that result in heat and noise generation. In addition, stiction, friction, compliance and backlash in these transmissions add highly nonlinear dynamics to mechanisms. Cobotic transmissions utilizing bearing quality steel components in dry-friction rolling-contact have none of these nonlinearities.

The authors would like to acknowledge the support of the Department of Energy, grant number DE-FG07-01ER63288.

E. L. Faulring is with the Mechanical Engineering Department, Northwestern University, 2145 Sheridan Road, Evanston, IL 60208 USA (phone: 847-467-1070; fax: 847-491-3915; e-mail: e-faulring@northwestern.edu).

J. E. Colgate and M. A. Peshkin are with the Mechanical Engineering Department, Northwestern University, 2145 Sheridan Road, Evanston, IL 60208 USA (e-mail: colgate@northwestern.edu, peshkin@northwestern.edu).

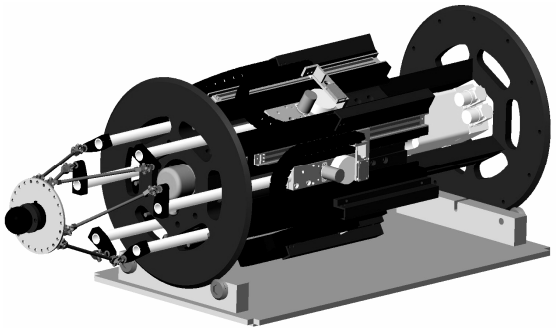

Figure 1. The Cobotic Hand Controller, a six-degree-of-freedom haptic display. An operator interacts with the spherical manipulandum at left. The device can display an extremely large range of impedances due to its use of continuously variable transmissions in its parallel architecture.

Using a continuously variable cobotic transmission can eliminate the need to make compromises on output flow and effort, which are inherent to choosing a fixed transmission ratio, and also allow the power actuator to be operated at an efficient speed nearly all of the time. Due to low power consumption and low weight requirements of prosthetics, large transmission ratios are often necessary in order to reduce an actuator's size for a given output effort, and in the case of electrical motors, allow them to operate at higher more efficient speeds. Unfortunately, the large transmission ratio reduces the maximum achievable output speed.

Parallel cobot architectures require only one power actuator for an unlimited number of degrees of freedom. The actuators that modulate the transmissions for each degree of freedom can be extremely small and low power, often an order of magnitude smaller than the single power actuator. The transmissions draw power from a single power actuator as needed, thus reducing the weight and power requirements of the mechanism. Only one set of high power electronics and drive-train components are needed.

With cobotic architecture, no electrical power is expended to resist forces in constrained directions. Electrical power is spent only to provide effort along the current motion direction. Rolling constraints in the transmission elements, not electrical power, resist forces orthogonal to the current motion direction. Only transmissions involved in the current motion direction draw off power from the single power actuator.

A continuously variable cobotic transmission also provides the ability to clutch the actuator, or conversely, to make it backdrivable. Prosthetics and rehabilitation robotic devices often have clutches that are engaged when switching from active to locked modes in order to provide high output efforts in the absence of output or input flows. However, these clutches hamper precise control of speed when

engaging and disengaging. Cobot transmissions exhibit this clutching ability without the need for an additional clutch mechanism. Since cobotic transmissions can be continuously varied between positive and negative ratios for a constant input speed, they can act as a clutch or brake when set to a zero ratio. Conversely, the transmission can be set to an infinite ratio, which effectively decouples the outputs from the input, therefore putting the mechanism in a passive, backdrivable mode.

Cobotic transmissions have a built in safety feature as well. Since they rely on frictional contacts to transmit power, the preload force at these contacts can be set to slip when a certain output force is exceeded.

In Section II of this paper we review the general design of the Cobotic Hand Controller. In Section III we provide an analysis of the efficiency of the rolling-contact portion of the rotational-to-linear transmissions. In Section IV we provide a comparison of the power efficiency of a cobotic system with that of a conventional electro-mechanical system for constant power throughputs. In Section V we provide a comparison of the power efficiency of the two systems for sinusoidal power throughputs across a range of frequencies.

II. The Cobotic Hand Controller

We introduce the six degree-of-freedom Cobotic Hand Controller here to illustrate how cobotic transmissions allow for the coupling of a high number of degrees of freedom to a single power source. This device uses six continuously variable transmissions to relate its six linear joints to a common rotating power source.

The design of the Cobotic Hand Controller, shown in Figure 2, utilizes the kinematics of a parallel platform introduced by Merlet and is discussed in much greater detail in [2, 4]. The proximal links, constrained to move linearly, parallel to the axis of the cylinder, are coupled by three-degree-of-freedom universal joints to the distal links, and these in turn are coupled via two-degree-of-freedom universal joints to an end-effector platform. Here a six-axis force-torque sensor is placed to determine the user's intent. Our addition to Merlet's kinematics has been to couple the six linear actuators to a central power cylinder through non-holonomic constraints, or steered rolling wheels.

Linear actuation of the proximal links is achieved via a rotational-to-linear continuously variable transmission (CVT), a steered wheel loaded against the surface of the cylinder. The Cobotic Hand Controller uses steel wheels that are the centers of plain spherical bearings with hardness Rockwell C 58, rolling on a Rockwell C 60 precision ground steel cylinder. This is in contrast to previous cobots that have utilized relatively compliant polyurethane Rollerblade™ wheels in order to obtain the necessary transverse coefficient of friction. The compliant wheels of previous cobots limited both their bandwidth and efficiency, proved an undesirable source of compliance, and allowed significant creep.

In Figure 3, the mechanism relating one of the six CVT wheels to its respective proximal link is shown. The angle of each wheel relates the linear velocity v_i of each proximal link to the rotational velocity of the power cylinder ω. Note that the wheels are only steered, not driven. The single cylinder is driven beneath them.

When the wheels are steered such that their rolling axis is parallel to the power cylinder ($\phi_i = 0$), a ratio $v_i/(r\omega) = -\tan(\phi_i) = 0$ is set. If the wheels are steered either direction from $\phi_i = 0$, ratios between $\pm$ infinity can be achieved. In practice, wheel slip limits the range to approximately ± 5. It is also evident that turning all six wheels to $\phi_i = 0$ locks the six actuators, and turning them to $\phi_i = \pi/2$ completely decouples the actuators from the cylinder's velocity, although the cylinder would then be unable to turn. Steering wheel i to $\phi_i = 0$ effectively clutches joint i. No additional clutch mechanism is required to do this. Finally, if the linear force f_i on a proximal link exceeds the product of the preload force on the respective CVT wheel with the coefficient of friction, $f_i > \mu N_i$, the wheel will slip, a behavior we use as a safety feature.

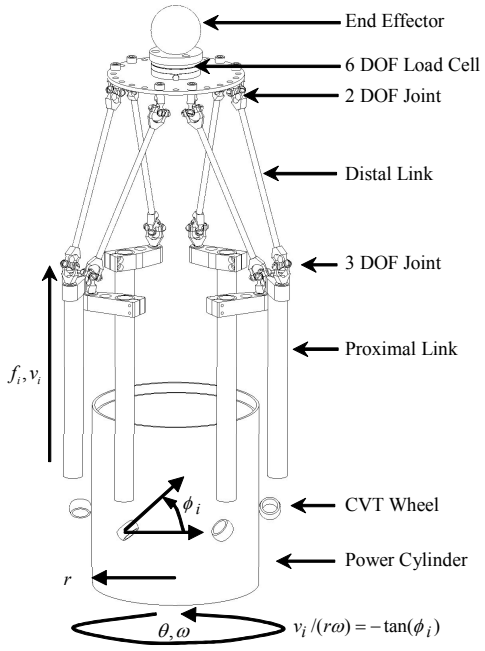

Figure 2. The kinematics of a Merlet-Cobotic parallel platform (not to scale). This design consists of six linear actuators arrayed around a central power cylinder. Figure 3 details the structure connecting the CVT wheels to the proximal links.

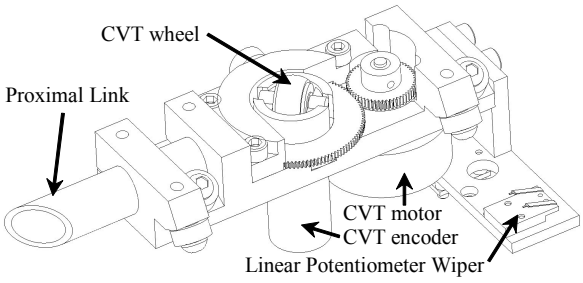

Figure 3. Mounted on the carraige is a steering assembly, consisting of a wheel preloaded via Belleville washers, an optical encoder, a steering motor coupled via gears and a wiper for a linear potentiometer.

In order to have the ability to vary the six transmission ratios independently, six CVT steering motors are required, along with the power cylinder motor, for a total of seven actuators for a six-degree-of-freedom mechanism. Although seven actuators are present, the end-effector of the Cobotic Hand Controller has only one instantaneous motion freedom due to the six rolling constraints, provided none of the steering actuators are set to $\phi_i = \pi/2$. The six transmissions steer this single motion freedom. The power cylinder conveys power along this one instantaneous motion freedom. The power cylinder does not need to expend any effort to resist output effort in the constrained directions orthogonal to the single motion freedom, as the rolling constraints of the preloaded wheels passively provide this force.

One should note that there is not a unique solution to the angles of the CVTs and the velocity of the power cylinder needed to create a certain end-effector velocity. It is arbitrary whether to operate the device with the cylinder spinning constantly, even when the end-effector is at rest, or to operate with the cylinder's velocity in some relationship to end-effector velocity. Since the ratio of end-effector speed to cylinder speed is arbitrary, it is at the designer's disposal to adjust for various haptic environments or to optimize given power consumption requirements. The mechanism's back-drivability, or lack thereof, is at our control to exploit via the CVTs. Even if all joints are clutched, energy can still be stored in the rotating cylinder to be drawn off later. Or, since the cobotic architecture can be made backdrivable by adjusting the ratios, one could envision a regenerative system.

Haptic simulations have unusual realism when displayed on the Cobotic Hand Controller. The smooth rigid feeling of the constraints that the Cobotic Hand Controller displays can not easily be expressed in plots of data, and is in stark contrast to the completely transparent freedom of motion the device can simulate when not in contact with virtual constraints. While traditional admittance displays can impart rigid constraints, and impedance displays excel at low impedance during free motion, few mechanical architectures exhibit the dynamic range of impedances achievable with cobotic transmissions utilizing steel elements in rolling-contact. Although the Cobotic Hand Controller is controlled as an admittance device, sensing forces with a load cell and rendering motions, the cobot does not suffer from the high inertia, friction and backlash that normally exist in a highly geared admittance device and is therefore not as limited in the range of impedances it can represent. Contrast the 20-400 kN/m achievable stiffness of the Cobotic Hand Controller to the 1 to 15 kN/m of achievable stiffness for traditional impedance displays [2]. Also contrast the 0.25 Kg simulated mass of the Cobotic Hand Controller's end-effector to the several Kg minimum masses specified for many admittance and some impedance displays [3]. The Cobotic Hand Controller has force transmission capabilities exceeding 50 N, structural stiffness ranging from 20-400 kN/m and a translational workspace of a 17 cm sphere [2].

III. Rotational-To-Linear Transmission

A. Bond Graph of a Rotational-to-linear Cobotic System

In order to further the analysis of the rotational-to-linear transmission, we develop a bond graph following the mechanical and electrical power flows in our rotational-to-linear transmission. In the remainder of this section we examine only the rolling-contact reduction element of the transmission. The other portions of this bond graph will be used in Sections IV and V to analyze the static and dynamic efficiencies of the overall cobotic transmission system.

The rotational-to-linear transmission, or cobotic drive-train, consists of a steering plant and a transmission plant as depicted in Figure 4. The drive-train is actuated by power cylinder electrical current $I_{cyl\ motor}$ and steering motor electrical current $I_{cvt\ motor}$, each driven by their respective voltage efforts. The drive-train's output is the flow v of the mass M_{load} and the effort f required to drive it.

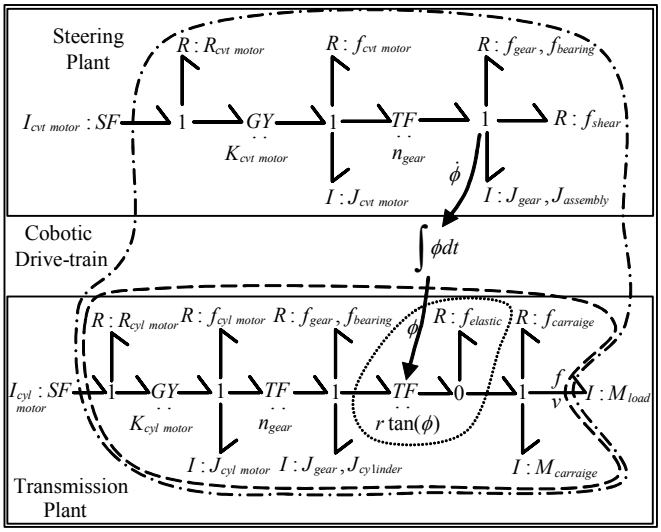

Figure 4. A bond graph of the rotational-to-linear cvt as it is considered in this analysis. The boundaries across portions of the steering plant and transmission plant define the input and output power flows for our efficiency calculations. Moving from left to right in the steering plant, the junctions represent power flow to electrical resistance of the steering motor, the conversion of electrical power to mechanical power, losses to inertia and friction of the steering motor, a gear reduction (≈ 2.5), losses due to inertia and friction of the gear reduction and assembly housing the cobot wheel as well as f_{shear}, the steering friction at the contact patch. Moving from left to right in the transmission plant, the junctions represent power flow to electrical resistance of the cylinder motor, the conversion of electrical power to mechanical power, losses due to inertia and friction of the cylinder motor, a gear reduction (≈ 58), losses due to inertia and friction of the gear and cylinder, a conversion of rotational power to translational power modulated by the cobot wheel steering angle ϕ, losses due to rolling-contact between elastic bodies $f_{elastic}$, and losses due to the friction and inertia of the linear carriage housing the steering plant.

B. Rolling-Contact Reduction Element Analysis

In studying the efficiency of the rotational-to-linear transmission, we first isolate the rolling-contact reduction

element itself and ignore the pre and post reduction element dynamics and/or losses. We assume that a ratio and therefore a steering angle ϕ has been set, and that the cylinder is rotating at a fixed velocity. Thus the only loss in the plant is $f_{elastic}$ which manifests itself in terms of longitudinal and lateral creeps, along and transverse to the rolling direction of the wheel, respectively.

The computation of $f_{elastic}$ is completed using the contact mechanics of linear elastic media in rolling-contact [5]. This model predicts lateral and longitudinal creep velocities as a function of lateral and longitudinal forces being transmitted through the contact patch of a rolling wheel. Figure 5 displays the theoretical predictions of efficiency and experimental efficiency data from the Hand Controller Cobot for the rolling-contact reduction elements. The experiment and theoretical model is carried out for a large range of transmission ratios, $\tan(\phi)$, and for two values of the ratio of output force relative to preload force, $f/(\mu N)$. N is the preload force on the CVT wheel, and μ the coefficient of friction between the wheel and cylinder.

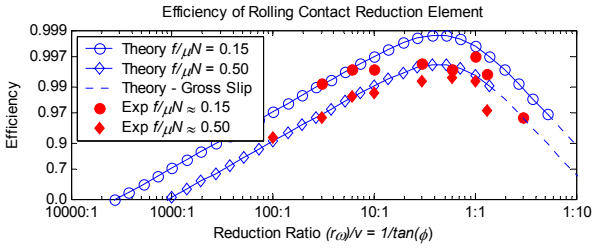

Figure 5. Theoretical versus experimental efficiency of the rolling-contact reduction element of the cobotic transmission. The linear creep theory should and does begin to fail at ratios smaller than 1:1, and the experimental efficiencies fall away from the predicted values as gross-slip between the rolling elements is approached. Experimental efficiencies are not reported for reduction ratios larger than 100:1 since accurate measurements become a confounding issue, although the device is capable of rendering ∞:1 ratios, or a completely clutched state.

The experimental protocol to isolate the efficiency of the rolling-contact reduction element is as follows. The steering plant fixes a transmission angle ϕ a priori. Thus an effective reduction ratio $\tan(\phi)$ between cylinder surface speed $r\omega$ and linear speed v is set. Subsequently, the efficiency of the rolling-contact reduction element is the mechanical power required to lift a known mass less the measured linear friction, divided by the electrical power required to turn the cylinder less the measured rotational friction. Since the system is operating at a constant velocity, no power flows to the inertias or to the steering plant.

Efficiency decreases with increased output force as the wheel begins to suffer more and more longitudinal and lateral creep during rolling-contact. Nevertheless, at 50 percent of peak output force, $f/\mu N = 0.5$, the transmission is 90 percent efficient even at a 100:1 gear ratio, and 99 percent efficient near a 1:1 gear ratio.

We compare these efficiencies to other types of gear trains in Figure 6. Planetary gear trains for low torque applications, harmonic drives, and worm gears have much lower efficiencies for a given reduction ratio that the cobotic rolling-contact reduction element. Also note that the reported efficiencies for gears are usually at peak continuous power throughput, where friction losses are smallest relative to the power throughput. Only very expensive very high torque planetary gear trains, not useful for prosthetics, or single gear pairs can achieve efficiencies above 90 percent.

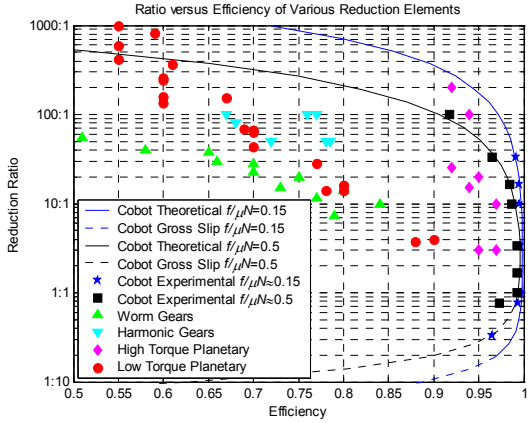

Figure 6. Efficiency of the rotational-to-linear rolling-contact reduction element versus conventional gears sampled at random from the internet.

IV. Static System Analysis

A. Introduction

In this section we develop a model of a conventional electro-mechanical linear-actuator, and compare the power efficiency of that drive-train to the complete cobotic drive-train. We compare the efficiency of the two actuation systems for static, constant force constant velocity outputs.

B. A Conventional Electro-mechanical Drive-train

We define a conventional system as a rotational electrical motor coupled through a gear-train to a pulley or capstan drive, in order to apply force f and affect the velocity v of the same mass M_{load} that the cobotic drive-train is coupled to. The bond graph we utilize to describe this conventional transmission plant is shown in Figure 7.

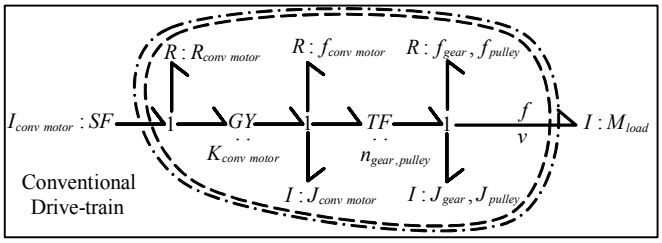

Figure 7. A bond graph of a conventional transmission plant, utilizing a rotational electric motor and a pulley to creat linear motion. Moving from left to right the junctions represent power flow to electrical resistance of the motor, the conversion of electrical power to mechanical power, losses due to inertia and friction of the motor, a gear reduction (≈ 3) and pulley radius (converts rotation to translation), and losses due to inertia and friction of the gear and pulley. The same linearly moving load M_{load}, as in the cobotic system, is driven by this conventional system at velocity v via force f.

C. *Desired Operating Regime*

In order to develop a fair comparison between the power efficiency of conventional and cobotic systems, we first define a common set of design goals, or a desired operating regime in the force f versus velocity v plane. A designer of a linear actuation system will likely specify a maximum force required, a maximum velocity required and also specify a maximum power that is expected at any given time. Thus a boundary in the force-velocity plane is developed from these three specifications like the desired operating regime boundary given in Figures 8 and 9.

D. *Static Performance of a Conventional Drive-train*

In Figure 8 we show the performance capabilities of various conventional electro-mechanical drive-train designs. The losses of these systems are the electrical resistance of the motor, and friction in the motor and gear-train. Since we are operating at constant force and constant velocity, no power flows into inertial components. Although Motor 1 is paired with several different gear ratios, it cannot achieve the maximum force and maximum velocity specifications simultaneously. It has no trouble developing the required power specification, but cannot do so across the range of operating conditions. In order to meet the maximum force and velocity specifications for a single gear ratio, a much larger Motor 2 must be selected, that has much more power capability than will ever be needed. Given that Motor 2's power capability is larger than needed, it never operates at maximum power, and therefore does not operate at high efficiency. Much of the electrical power is lost to resistive heating of the motor windings as it operates at inefficient speeds. Although the combination of Motor 2 and the gearing is capable of 85 percent power efficiency, it never exceeds 65 percent efficiency in our desired operating regime.

E. *Static Performance of a Cobotic Drive-train*

In a static analysis of the cobotic drive-train, we are concerned with the efficiency of the transmission plant in the absence of any steering action. Thus a steering angle has been set and no electrical flow $I_{cvt\ motor}$ is required in order to maintain the angle of the CVT. We therefore consider the power efficiency across the boundary drawn in Figure 4, which is the mechanical power flowing into M_{load} divided by the electrical power driving the cylinder motor. The losses consist of the dissipation due to elastic bodies in rolling-contact, $f_{elastic}$, the resistive and frictional losses of the cylinder motor, the frictional losses of the gearset driving the cylinder, and the friction of the linear guide-way. No power flows into the inertias of the system since we are holding the velocity constant. Likewise, no power flows to the steering plant since the angle is fixed for constant force and constant velocity operating conditions.

Figure 9 displays theoretical predictions of this model for the cobotic system. The smaller Motor 1, although insufficient to meet our performance criteria in the conventional drive-train, is sufficient in the cobotic drive-train design. The cobotic drive-train's continuously variable transmission allows the capture of maximum power output of Motor 1 across all output forces and velocities. In addition, higher power efficiencies are reached by the cobotic drive-train than the conventional drive-train at a given f, v point, since the cobotic drive-train's motor is always operating at an efficient speed. Nevertheless, the significant gear reduction between the cylinder motor and the cylinder limits the cobotic drive-train's efficiency to 70 percent.

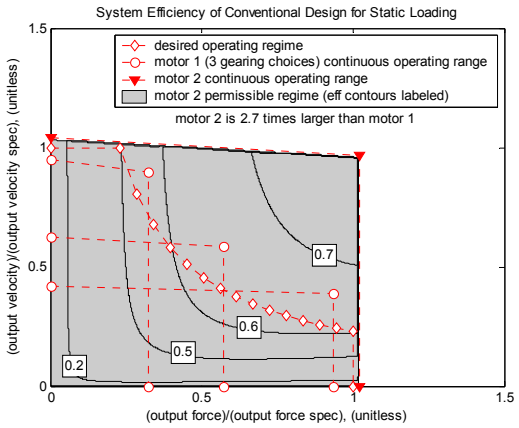

Figure 8. The ranges of operation of some conventional drive-train designs, and contours of power efficiency of the Motor 2 design. The right hand boundary of the continuous operating regimes is limited by the continous torque that a motor can develop without overheating. The sloping upper boundary is the maximum velocity that a motor can be driven at, considering the torque requirement. This sloping boundary would intersect the horizontal axis at the momentary peak torque achievable by the motor.

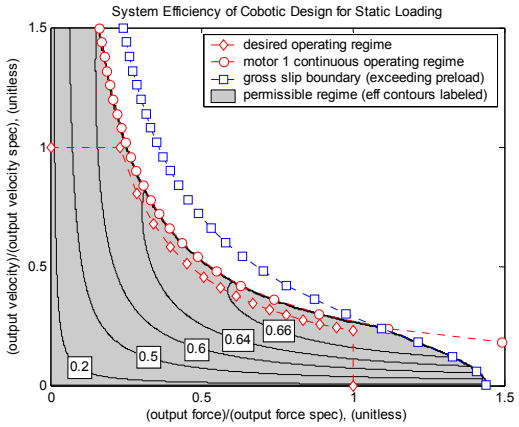

Figure 9. The range of operation of a cobotic drive-train using the same Motor 1 as the conventional drive-train design in Figure 8. Note the much higher power efficiencies at high forces and low velocities of the cobotic versus the conventional drivetrain. The velocity limit of Motor 1 is not an issue since it is operating constantly at its most efficient speed. However, the operating regime is still limited by the continous torque that Motor 1 can apply at its efficient speed. The torque requirement of the motor for a given f and v is predicted by selecting the steering angle to meet the velocity, $\phi = \text{atan}(v/(r\omega))$, and then computing the cylinder torque required to provide the force, $\tau = r\tan(\phi)f$. The boundaries in Figure 9 also consider all the other requirements of the complete bond graph given in Figure 4. The non-normal loads on the contact patch between the wheel and cylinder is a function of f and $\phi = \text{atan}(v/(r\omega))$, and exceeding the normal preload μN leads to the gross slip boundary shown in the figure.

V. Dynamic System Performance

In a dynamic analysis we are concerned with the net efficiency of the linear actuation system throughout the course of acceleration and deceleration, and for the cobotic system, the presence of steering action. Thus additional power is required to steer the wheel or modulate the transmission, and to accelerate and decelerate inertias in each drive-train. The boundaries for dynamic analysis shown on the bond graphs in Figures 4 and 7 show the losses we consider.

Figure 10 shows a comparison of the system efficiencies across a range of frequencies and a range of fraction of maximum specified power throughput. In order to create a fair comparison, we choose a common inertial load M_{load} for each linear system to move in a sinusoid. Then, given a frequency of operation and a fraction of the maximum power specification, an amplitude of motion is computed. Each system is put through one cycle of this motion and the desired output power is divided by the electrical power requirements to yield the dynamic power efficiency of the systems.

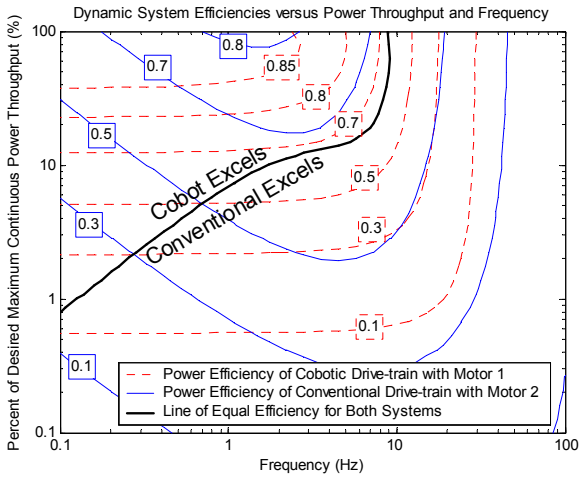

Figure 10. Comparison of the power efficiency contours of cobotic drive-trains and conventional drive-trains at driving a mass sinusoidally. Given a load to be oscillated linearly at a certain frequency, various amplitudes of motion were chosen that utilized a given fraction of the desired rms power throughput, one of our design specifications. The conventional drive-train requires the larger Motor 2 to meet the design specifications, while the cobotic drive-train suffices with the smaller Motor 1. Both drive-trains can achieve higher efficiencies in the dynamic case than the static loading scenario because frictional losses do not detract from dynamic efficiency, since friction helps the system decelerate the load, just as much as it hinders the acceleration phase.

In general, the cobotic drive-train has higher power efficiency than the conventional drive-train at less than 10 Hertz and greater than 10 percent of the maximum power throughput. In this regime, the cobot is losing power to high gear reduction and friction, but the conventional drive-train is losing most of its power to electrical resistance. At mid-range frequencies of voluntary human motion, one to ten hertz, the two drive-train types have relatively similar power efficiencies, even with the expenditure of the cobot to modulate the steering angle. Yet the cobotic transmission has the additional ability to act as a clutch or become backdrivable, and can have a single smaller power actuator for numerous degrees of freedom. We also see much room for improvement in the dynamic efficiency of our current cobotic design, by reducing the rotational inertia and bearing friction of the steering plant, and by reducing the mass of the linearly moving steering plant. Both systems show increasing efficiency with increasing power throughput. Both systems also exhibit decreasing efficiency at high frequencies since they expel effort to accelerate and decelerate inertias in the drive-trains, in addition to the load.

VI. Conclusion

A novel cobotic device is reviewed that demonstrates the attractive properties of low weight and low power consumption. The device is capable of rendering both solid smooth constraints and transparent freedom of motion. The crisp distinction between free and forbidden directions of motion is a salient feature of cobots. This performance arises not from elaborate control algorithms, but from the inherent physical characteristics of the device due to the utilization of non-holonomic rolling constraints in its transmissions.

The device's parallel cobotic architecture features continuously variable transmissions, variable back-drivability, high efficiency, no need for brakes or clutches, precise control of output force and velocity at low output speeds, and a single power actuator for multiple degrees of freedom. Through an extensive comparative analysis, a cobotic rotational-to-linear actuator is shown to require a smaller power actuator, and have comparable if not higher power efficiencies than a conventional electro-mechanical linear actuator for frequencies of voluntary human motion.

The analysis in this paper is for frequency characteristics of voluntary human motion, typically at or below ten hertz. Separate research to be published in the future analyzes the performance of the rotational-to-linear CVT at higher frequencies such as those expected from a haptic display.

References

[1] M. A. Peshkin, J. E. Colgate, W. Wannasuphoprasit, C. A. Moore, R. B. Gillespie, and P. Akella, "Cobot architecture," IEEE Transactions on Robotics and Automation, vol. 17, pp. 377-390, 2001.

[2] E. L. Faulring, J. E. Colgate, and M. A. Peshkin, "A high performance 6-DOF haptic cobot," in Proc. IEEE International Conference on Robotics and Automation, New Orleans, LA, 2004, 1980-1985.

[3] E. L. Faulring, K. M. Lynch, J. E. Colgate, and M. A. Peshkin, "Haptic interaction with constrained dynamic systems," in Proc. IEEE International Conference on Robotics and Automation, Barcelona, Spain, 2005.

[4] J. P. Merlet, "Direct kinematics and assembly modes of parallel manipulators," International Journal of Robotics Research, vol. 11, pp. 150-162, 1992.

[5] K. L. Johnson, Contact Mechanics. Cambridge, U.K.: Cambridge University Press, 1985.